Streamlined synthesis of C(sp³)–H rich *N*-heterospirocycles enabled by visible-light-mediated photocatalysis

Nils J. Flodén[1], Aaron Trowbridge[1], Darren Willcox[1], Scarlett M. Walton[1,2], Yongjoon Kim[1] & Matthew J. Gaunt*[1]

[1]Department of Chemistry, University of Cambridge, Lensfield Road, Cambridge CB2 1EW, United Kingdom, UK
[2] Medicinal Chemistry, Oncology, IMED Biotech Unit, AstraZeneca, Cambridge, UK

Supporting Information Placeholder

ABSTRACT: We report a general visible light-mediated strategy that enables the construction of complex C(sp³)-rich *N*-heterospirocycles from feedstock aliphatic ketones and aldehydes with a broad selection of alkene-containing secondary amines. Key to the success of this approach was the utilization of a highly-reducing Ir-photocatalyst and orchestration of the intrinsic reactivities of 1,4-cyclohexadiene and Hantzsch ester. This methodology provides streamlined access to complex C(sp³)-rich *N*-heterospirocycles displaying structural and functional features relevant to fragment-based lead identification programs.

Growing evidence suggests that an increasing number of aromatic rings in lead compounds can result in greater attrition rates amongst pharmaceutical candidates due to poor solubility, bioavailability and pharmacokinetics.[1] However, libraries of lead-like structures often comprise compounds with predominantly C(sp²)-rich scaffolds. Consequently, the assessment of structurally distinct libraries of C(sp³)-rich small molecules displaying diverse polar functionality could help to identify new lead candidates in fragment-based screening approaches that may exhibit enhanced physical and biological properties.[2] In considering the design of novel C(sp³)-rich small molecules for fragment-based approaches,[3] it is noticeable that conformationally restricted scaffolds show highly reproducible results in *in silico* screening programmes; the well-defined spatial orientation of molecular features in a candidate compound often leads to increased binding affinities. One approach towards limiting structural flexibility within C(sp³)-rich small molecules is through the introduction of a spirocycle.[4] In comparison to aromatic scaffolds, fine-tuning the structural and functional features in these frameworks offers an alternative means through which to probe interactions with target binding sites by variation of ring size, adjusting electronic properties and manipulating substituent effects.[5] As a result, spirocyclic motifs displaying polar functionality are emerging in pharmaceutical agents and lead compounds (Figure 1a).[4]

Despite the attractive properties offered by rigid saturated polar spirocyclic scaffolds, access to diversely functionalized variants mainly relies on multistep alkyl- and acylative methods.[5] Notable advances on these approaches

include dearomatization-based strategies, using Pd, Ir or Fe catalysts,[6a-c] which harness the intrinsic reactivity of tethered (hetero)arene building blocks for the generation of a selection of spirocyclic *N*-heterocycles with different ring sizes. Bode and co-workers produced a range of spirocyclic *N*-heterocycles using their SnAP technology;[6d,e]

Figure 1. The evolution of the cyclization strategy
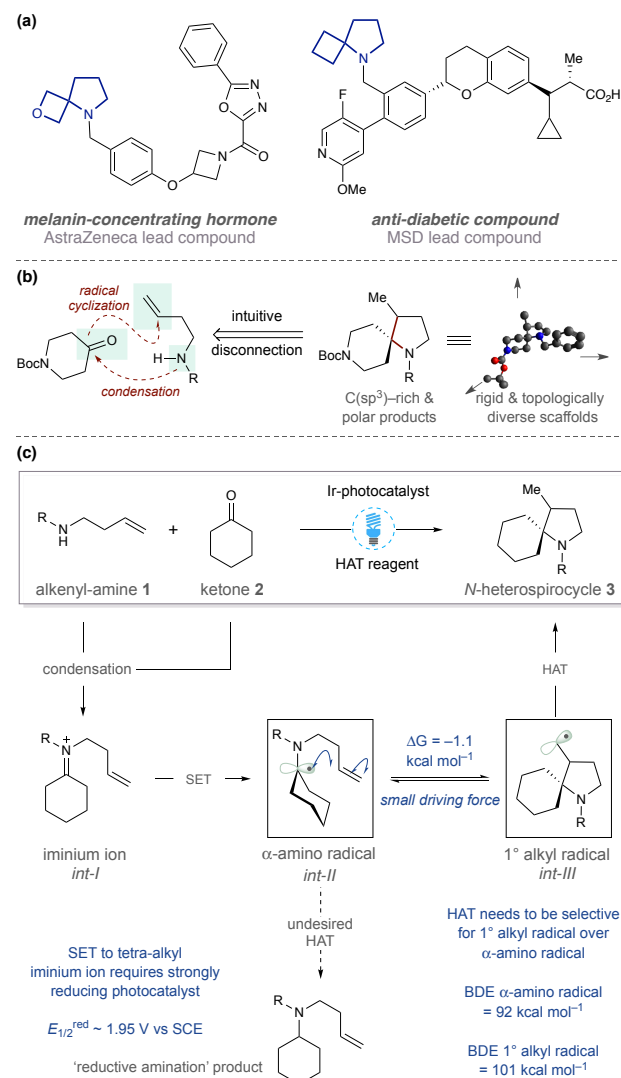
Gibbs free energy calculated by DFT-methods (UPW6B95-D3BJ/def2-QZVP). Hydrogens removed for clarity.

iminium ion formation between amino-stannane reagents and cyclic ketones enables a stoichiometric copper(II)-triggered cyclization to access free(NH)-secondary amino-spirocyclic products. To complement these approaches, we reasoned that a photocatalytic strategy[7] based on an intuitive retrosynthetic disconnection of tertiary amine-based *N*-heterospirocycles directly to feedstock ketones and readily available alkenyl-derived secondary amines could be realized through the intermediacy of an α-amino radical (Figure 1b).[8] The structurally distinct C(sp³)-rich polar *N*-heterospirocycles generated by such a catalytic transformation would be of great interest to practitioners of synthetic and medicinal chemistry.

We envisioned that visible-light-mediated photocatalytic single-electron reduction of an alkyl-iminium ion (*int-I*, Figure 1c), formed from the condensation of a saturated cyclic ketone with a secondary alkyl amine, would form a cyclic-tertiary α-amino radical (*int-II*). Addition of this α-amino radical to an appended alkene on the amine component would give rise to a substituted pyrrolidine-based spirocyclic scaffold. Recent work from our group established a photocatalytic platform for the addition of nucleophilic α-amino radicals (formed from the corresponding iminium ions) to electron-deficient olefins.[9] Critically, however, a catalytic manifold for the addition of all-alkyl substituted α-amino radicals to unactivated alkenes remains an unsolved problem, principally due to the mismatched electronics and low thermodynamic driving force for such a reaction. The lone pair on the nitrogen atom stabilizes the α-amino radical but also renders it nucleophilic. Therefore, its addition to an unactivated alkene is polarity-mismatched and produces an alkyl radical (*int-III*) with no stabilizing substituents that, in turn, can undergo the reverse reaction to reform the α-amino radical via C–C bond β-scission. Indeed, the use of SmI₂, a strong stoichiometric reductant, was required to trap related alkyl radicals via organosamarium intermediates following addition to unactivated alkenes.[10] However, the metal waste produced in these reactions and frequent need for highly dilute conditions has hindered the wider application of this type of process.[11] We, therefore, questioned whether an alkyl radical could be selectively intercepted in a milder fashion by way of a hydrogen-atom transfer (HAT) reaction and in preference to HAT to the α-amino radical.

Herein, we detail the successful realization of these ideas through the development of a streamlined strategy for the synthesis of complex C(sp³)-rich *N*-heterospirocycles from readily available secondary amines and ketones enabled by visible-light photocatalysis. Key to the success of this strategy was the utilization of a highly reducing Ir-photocatalyst and orchestrating the intrinsic reactivities of 1,4-cyclohexadiene and Hantzsch ester, which facilitated controlled generation and fate of the radical intermediates present in the reaction. Under optimized conditions, the process combines a range of feedstock aliphatic ketones and aldehydes with alkene-containing secondary amines to forge complex C(sp³)-rich *N*-heterospirocycles displaying structural, functional and physical features that are likely to be attractive in fragment-based lead identification programs.

We began our investigations by testing reaction conditions based on our previously established photocatalytic process.[9] Using amine **1a** and cyclobutanone (**2a**) as substrates, 1mol% of Ir(ppy)₃ and 2.0 equivalents of Hantzsch ester, we were encouraged by the formation of spirocycle **3a** in 30% yield and only trace amounts of the corresponding reductive amination product (Table 1, entry 1). Following extensive optimization, we found that the use of 1,4-cyclohexadiene as an additive (entry 2) and a more reducing photocatalyst Ir(dMeppy)₃ ([$E_{1/2}^{red}$(Ir^{IV}/*Ir^{III})]= −1.86 V vs SCE in CH₂Cl₂) (entry 3) improved the yield to 97%.[12] We reasoned that the use of 1,4-CHD as a HAT-donor in high concentration would restrict the role of Hantzsch ester to turning over the Ir(IV) species formed after single-electron reduction of the iminium ion, while the more reducing photocatalyst would provide a stronger driving-force for the reduction step. A series of control experiments showed that the yield of the reaction dropped to 24% in the absence of 1,4-CHD (entry 4); to 43% without the Hantzsch ester (entry 5); and to trace amounts without photocatalyst or light or in the absence of both 1,4-CHD and Hantzsch ester (entries 6,7).
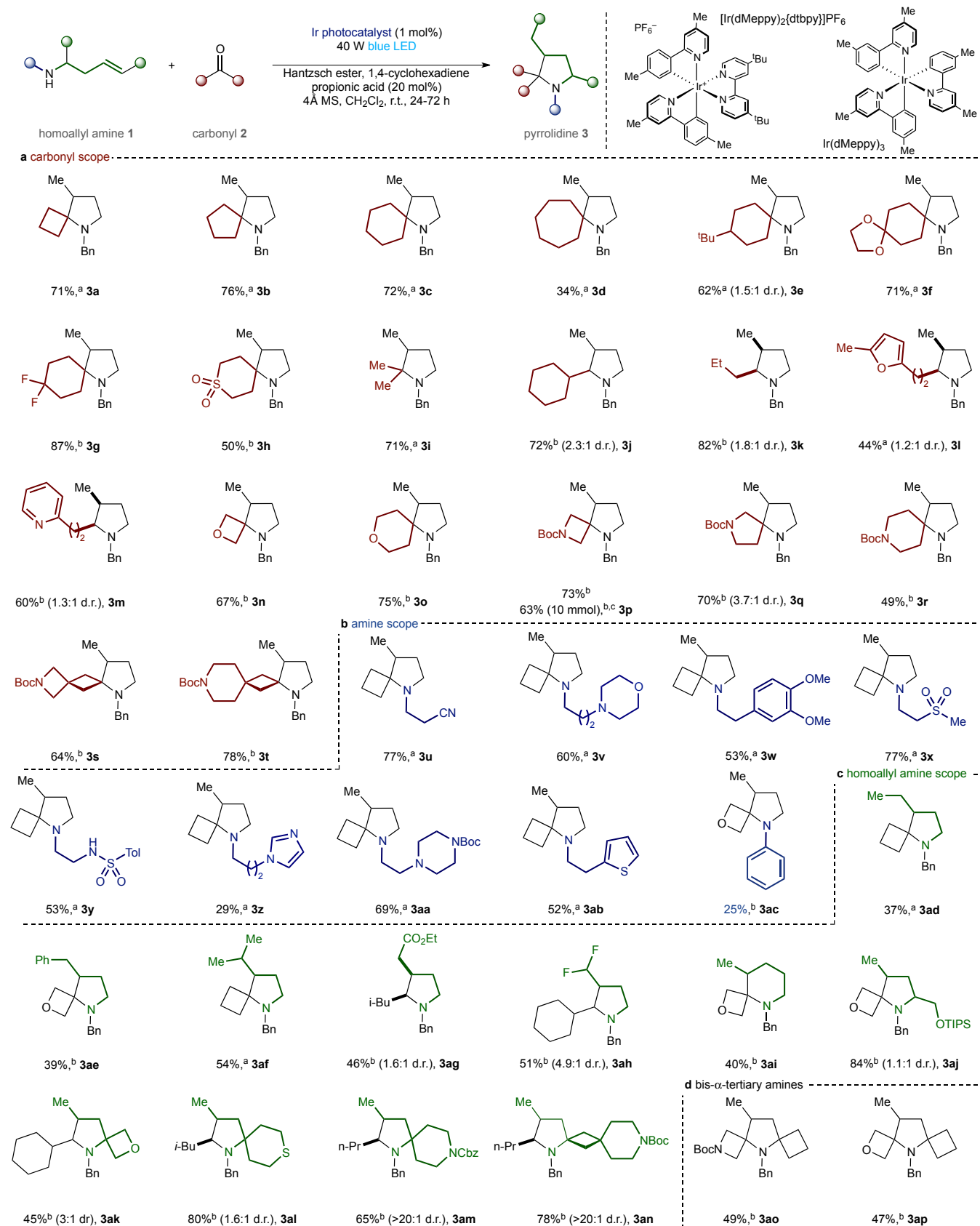
Table 1. Selected optimization data[a]

Entry	Catalyst	Hantzsch (equiv)	1,4-CHD (equiv)	Yield %
1	Ir(ppy)₃	2.0	–	30
2	Ir(ppy)₃	2.0	7.5	45
3	Ir(dMeppy)₃	2.0	7.5	97
4	Ir(dMeppy)₃	2.0	–	24
5	Ir(dMeppy)₃	–	7.5	43
6		2.0	7.5	trace
7	Ir(dMeppy)₃	–	–	trace

[a]Reactions employed a 40 W Blue Kessil lamp & yields calculated by GC assay with dodecane as internal standard.

Having evaluated the reaction conditions, a range of commercially available ketones (Table 2) were reacted to afford *N*-heterospirocycles **3a-3i**. Aldehydes also reacted to afford the corresponding pyrrolidines (**3j-3m**), with the *syn*-isomer of **3k** being the major diastereomer. The reaction was amenable to heterocyclic ketones, with a series of saturated *N*-heterocyclic readily transformed into rigid, C(sp³)-rich and polar bis-*N*-heterospirocyclic scaffolds with orthogonal protecting groups on the two nitrogen atoms (**3n-t**), facilitating further derivatization. The reaction to form azetidine-derived spirocycle **3p** could be performed on a gram-scale, even with a reduced catalyst loading of 0.5 mol%, forming the product in a 63% yield; the *N*-groups in **3p** could also be selectively deprotected for further derivatization.[13] Such derivatives are frequently employed as β-turn mimetics for GPCR protein binding where the orthogonality of the two nitrogen substituents is key to achieve the desired turn-characteristics.[14] While the Ir(dMeppy)₃ photocatalyst had proven optimal for reactions using electron-rich ketones (to form **3a-3e**, **3i**, **3l**), higher yields were observed for electron-deficient ketones (to form **3f-3h, 3j-3k & 3m-3t**) using the less-reducing [Ir(dMeppy)₂{dtbbpy}]PF₆ photocatalyst.
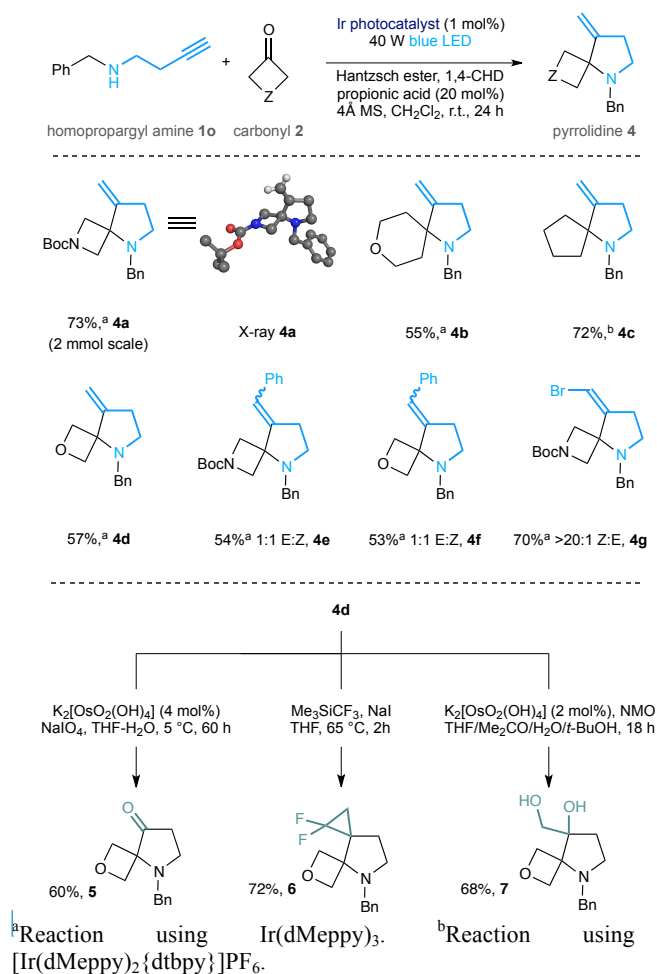
Table 2. Scope of photocatalytic synthesis of *N*-heterospirocycles.

a carbonyl scope

71%,[a] **3a**

76%,[a] **3b**

72%,[a] **3c**

34%,[a] **3d**

62%[a] (1.5:1 d.r.), **3e**

71%,[a] **3f**

87%,[b] **3g**

50%,[b] **3h**

71%,[a] **3i**

72%[b] (2.3:1 d.r.), **3j**

82%[b] (1.8:1 d.r.), **3k**

44%[a] (1.2:1 d.r.), **3l**

60%[b] (1.3:1 d.r.), **3m**

67%,[b] **3n**

75%,[b] **3o**

73%[b]
63% (10 mmol),[b,c] **3p**

70%[b] (3.7:1 d.r.), **3q**

49%,[b] **3r**

b amine scope

64%,[b] **3s**

78%,[b] **3t**

77%,[a] **3u**

60%,[a] **3v**

53%,[a] **3w**

77%,[a] **3x**

53%,[a] **3y**

29%,[a] **3z**

69%,[a] **3aa**

52%,[a] **3ab**

25%,[b] **3ac**

c homoallyl amine scope

37%,[a] **3ad**

39%,[b] **3ae**

54%,[a] **3af**

46%[b] (1.6:1 d.r.), **3ag**

51%[b] (4.9:1 d.r.), **3ah**

40%,[b] **3ai**

84%[b] (1.1:1 d.r.), **3aj**

d bis-α-tertiary amines

45%[b] (3:1 dr), **3ak**

80%[b] (1.6:1 d.r.), **3al**

65%[b] (>20:1 d.r.), **3am**

78%[b] (>20:1 d.r.), **3an**

49%,[b] **3ao**

47%,[b] **3ap**

[a]Reaction using Ir(dMeppy)₃. [b]Reaction using [Ir(dMeppy)₂{dtbpy}]PF₆. [c]0.5mol% [Ir].

We next assessed *N*-substituted alkenylamines, (**3u-3an**), where useful functional groups such as sulfonamide, *N*-Boc-piperidine, heteroaryl motifs (**3u-3ab**) and a less nucleophilic aniline (**3ac**) could be built into the spirocycle products. Substitution on the alkene was tolerated (**3ad-3ah**), introducing valuable functionality such the ester and *gem*-difluoro in useful yields. Whilst no cyclized product was observed from attempts at reacting *N*-benzyl allyl amine (to afford azetidine-based spirocycles), a piperidine scaffold **3ai** could be assembled via a 6-*exo* cyclization, further expanding scope of the process. Homoallylic amines containing α–substitutents were effective in the cyclization process with both aldehydes and functionalized alicyclic ketones, in some cases with surprisingly high diastereoselectivities **3aj-3an**. We found that the exceptionally hindered spirocycles **3ao & 3ap** could be accessed in 49% & 47% yield respectively, affording access to a class of compounds that are challenging to synthesize using classical C–N bond-forming methods.[6e,15,16]
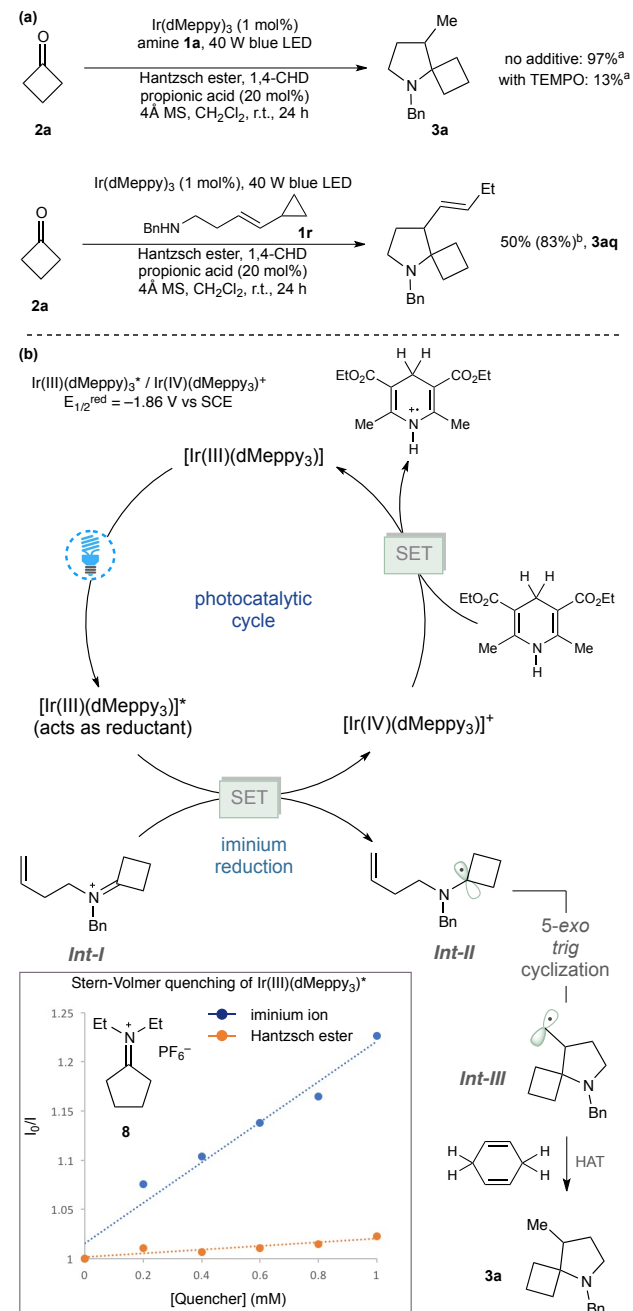
Figure 2. Cyclization on alkynes & amine derivatizations

homopropargyl amine **1o**   carbonyl **2**   pyrrolidine **4**

73%,[a] **4a** (2 mmol scale)   X-ray **4a**   55%,[a] **4b**   72%,[b] **4c**

57%,[a] **4d**   54%[a] 1:1 E:Z, **4e**   53%[a] 1:1 E:Z, **4f**   70%[a] >20:1 Z:E, **4g**

K_2[OsO_2(OH)_4] (4 mol%) NaIO_4, THF-H_2O, 5 °C, 60 h

Me_3SiCF_3, NaI THF, 65 °C, 2h

K_2[OsO_2(OH)_4] (2 mol%), NMO THF/Me_2CO/H_2O/*t*-BuOH, 18 h

60%, **5**   72%, **6**   68%, **7**

[a]Reaction using Ir(dMeppy)_3. [b]Reaction using [Ir(dMeppy)_2{dtbpy}]PF_6.

Next, we questioned whether we could apply the α-amino radical to a cyclization process with simple alkynes, affording *N*-heterospirocycles carrying a useful alkenyl handle for further functionalization. *N*-benzyl 4-aminobutyne derivatives smoothly reacted with a range of cyclic ketones furnishing the desired spirocycles **4a-g** in 53–73% yield

(Figure 2a). Finally, the alkenyl handle of **4d** could be derivatized through a difluorocyclopropanation to afford **6** in 72% yield, whose structure comprises three different sized ring-systems and two adjacent spirocyclic centres, as well as different oxidative transformations (**5 & 7**, Figure 2b).[17]

Figure 3. Mechanistic studies

(a)

Ir(dMeppy)_3 (1 mol%) amine **1a**, 40 W blue LED

Hantzsch ester, 1,4-CHD propionic acid (20 mol%) 4Å MS, CH_2Cl_2, r.t., 24 h

no additive: 97%[a] with TEMPO: 13%[a]

2a   **3a**

Ir(dMeppy)_3 (1 mol%), 40 W blue LED

BnHN   **1r**

Hantzsch ester, 1,4-CHD propionic acid (20 mol%) 4Å MS, CH_2Cl_2, r.t., 24 h

50% (83%)[b], **3aq**

2a

(b)

Ir(III)(dMeppy)_3* / Ir(IV)(dMeppy)_3^+ $E_{1/2}^{red}$ = −1.86 V vs SCE

[Ir(III)(dMeppy_3)]

photocatalytic cycle

[Ir(III)(dMeppy_3)]* (acts as reductant)

[Ir(IV)(dMeppy_3)]^+

SET

iminium reduction

Int-I

Int-II

5-*exo* trig cyclization

Int-III

HAT

3a

Stern-Volmer quenching of Ir(III)(dMeppy)_3*

8

[a]Yield determined by GC assay with dodecane as internal standard. [b]Yield determined by ^{1}H NMR with 1,1,2,2-tetrachloroethane as internal standard.

We found that the addition of TEMPO, as a radical trap, significantly inhibited the reaction (Figure 3a). A reaction with cyclopropyl-substituted alkenyl amine **1r** led to the ring opened product, supporting the existence of a cyclized radical intermediate (c.f. *Int-III*). Stern-Volmer studies on a representative iminium ion **8** showed effective quenching of the excited state of the Ir(dMeppy)_3 photocatalyst in

comparison to Hantzsch ester (Figure 3c). As a result of these studies and those outlined in our optimization (Table 1), we propose a tentative mechanism for the reaction which begins with visible-light excitation of Ir(dMeppy)$_3$ to Ir(dMeppy)$_3$* (Figure 3c). Single-electron reduction of the iminium ion (*Int-I*) by Ir(dMeppy)$_3$* forms the α-amino radical (*Int-II*), which engages the pendant alkene in a 5-*exo-trig* cyclization to form an alkyl radical (*Int-III*); HAT from 1,4-CHD to the alkyl radical then forms *N*-heterospirocycle **3**. The oxidized Ir(IV)(dMeppy)$_3$ species is reduced to the active catalyst by single-electron transfer from the Hantzsch ester, closing the catalytic cycle.

In summary, we have developed a visible-light mediated process to enable the facile synthesis of heterospirocyclic compounds from readily available starting materials. The photoredox strategy offers an intuitive retrosynthetic disconnection for difficult-to-access C(sp^3)-rich *N*-heterospirocyclic scaffolds that may be of interest to practitioners of both synthetic and medicinal chemistry.

ASSOCIATED CONTENT

The Supporting Information is available free of charge on the ACS Publications website. Experimental procedures and spectral data (PDF); crystallographic data (CIF)

AUTHOR INFORMATION

Corresponding Author

*mjg32@cam.ac.uk

ACKNOWLEDGMENT

REFERENCES

(1) (a) Lovering, F.; Bikker, J.; Humblet, C. Escape from flatland: increasing saturation as an approach to improving clinical success. *J. Med. Chem.* **2009**, *52*, 6752−6756. (b) Blakemore, D. C.; Castro, L.; Churcher, I.; Rees. D. C.; Thomas, A. W.; Wilson, D. M.; Wood, A. Organic synthesis provides opportunities to transform drug discovery. *Nat. Chem.* **2018**, *10*, 383−394.

(2) Murray, C. W.; Rees, D. C. The rise of fragment-based drug discovery. *Nat. Chem.* **2009**, *1*, 187−192.

(3) (a) Fang, Z.; Song, Y.; Zhan, P.; Zhang, Q.; Liu, X. Conformational restriction: an effective tactic in "follow-on"-based drug discovery. *Future Med. Chem.* **2014**, *6*, 885−901. (b) Wipf, P.; Skoda, E. M.; Mann, A. *The Practice Of Medicinal Chemistry. Chapter 11 – Conformational Restriction And Steric Hindrance In Medicinal Chemistry.* (Academic Press, San Diego, 2015).

(4) (a) Zheng, Y.-J.; Tice, C. M.; Singh, S. B. The use of spirocyclic scaffolds in drug discovery. *Bioorg. Med. Chem. Lett.* **2014**, *24*, 3673−3682. (b) Zheng, Y.-J.; Tice, C. M. The utilization of spirocyclic scaffolds in novel drug discovery. *Expert Opin. Drug Discov.* **2016**, *11*, 831−834. (c) Johansson, L.; Anders, M. Azetidine derivatives for treatment of melanin related disorders. Patent WO 2013/011285 A1, 2013. (d) Chen, H.; Colletti, S. L.; Demong, D.; Guo, Y.; Miller, M.; Nair, A.; Plummer, C.; Xiao, D.; Yang, D.-Y. Antidiabetic bicyclic compounds. Patent WO 2016/022742 A1, 2016.

(5) (a) Carreira, E. M.; Fessard, C. T. Four-membered ring-containing spirocycles: synthetic strategies and opportunities. *Chem. Rev.* **2014**, *114*, 8257−8322. (b) Rios, R. Enantioselective methodologies for the synthesis of spiro compounds. *Chem. Soc. Rev.* **2012**, *41*, 1060−1074. (c) Singh, F. V.; Kole, P. B.; Mangaonkar, S. R.; Shetgaonkar, S. E. Synthesis of spirocyclic scaffolds using hypervalent iodine reagents. *Belstein J. Org. Chem.* **2018**, *14*, 1778−1805. (d) Melnykov, K. P.; Artemenko, A. N.; Ivanenko, B. O.; Sokolenko, Y. M.; Nosik, P. S.; Ostapchuk, E. N.; Grygorenko, O. O.; Volochnyuk, D. M.; Ryabukhin. S. V. Scalable synthesis of biologically relevant spirocyclic pyrrolidines. *ACS Omega* **2019**, *4*, 7498−7515.

(6) (a) Rousseaux, S.; Garcia-Fortanet, J.; Angel Del Aguila Sanchez, M.; Buchwald, S. L. *J. Am. Chem. Soc.* **2011***, 133*, 9282−9285. (b) Zhu, M.; Zheng, C.; Zhang, X.; You, S-L. Synthesis of cyclobutane-fused angular tetracyclic spiroindolines via visible-light-promoted intramolecular dearomatization of indole derivatives. *J. Am. Chem. Soc.* **2019**, *141*, 2636−2644. (c) Adams, K.; Ball, A. K.; Birkett, J.; Brown, L.; Chappell, B.; Gill, D. M.; Tony Lo, P. K.; Patmore, N. P.; Rice, C. R.; Ryan. J.; Raubo, P.; Sweeney, J. B. An iron-catalysed C-C bond forming spiro-cyclization cascade providing sustainable access to new 3D heterocyclic frameworks. *Nat. Chem.* **2017**, *9*, 396−401. (d) Siau, W.-Y.; Bode, J. W. One-step synthesis of saturated spirocyclic *N*‾heterocycles with stannyl amine protocol (SnAP) reagents and ketones. *J. Am. Chem. Soc.* **2014**, *51*, 17726−17729. (e) Saito, F.; Trapp, N.; Bode, J. W. Iterative assembly of polycyclic saturated heterocycles from monomeric building blocks. *J. Am. Chem. Soc.* **2019**, *141*, 5544−5554.

(7) Prier, C.; Rankic, D.; MacMillan, D. W. C. Visible light photoredox catalysis with transition metal complexes: applications in organic synthesis. *Chem. Rev.* **2013**, *113*, 5322−5363.

(8) For reviews, see: (a) Zou, Y.-Q.; Xiao, W.-J. Visible light mediated α-amino C–H functionalization reactions, Chapter 4, 93−128, **2018**, Wiley-VCH. (b) Beatty, J. W.; Stephenson, C. R. J. Amine functionalization via oxidative photoredox catalysis: methodology development and complex molecule synthesis. *Acc. Chem. Res.* **2015**, *48*, 1474 *Acc. Chem. Res.* **2015**, *48*, 1474−1484. (c) Nakajima, K.; Miyake, Y.; Nishibayashi, Y. Synthetic utilization of α-aminoalkyl radicals and related species in visible light photoredox catalysis. *Acc. Chem. Res.* **2016**, *49*, 1946−1956. For selected examples, see: (d) McNally, A.; Prier, C.; MacMillan, D. W. C. Discovery of an α-amino arylation reaction using the strategy of accelerated serendipity. *Science* **2011**, *334*, 1114−1117. (e) McManus, J. B.; Onuska, N. P. R.; Nicewicz, D. A. Generation and alkylation of α-

carbamyl radicals via organic photoredox catalysis. *J. Am. Chem. Soc.* **2018**, *140*, 9056–9060. (f) Zuo, Z.; Ahneman, D. T.; Chu, L.; Terrett, J. A.; Doyle, A. G.; MacMillan, D. W. C. Merging photoredox with nickel catalysis: coupling of α-carboxyl sp³-carbons with aryl halides. *Science*, **2014**, *345*, 437–440. (g) Shaw, M.; Shurtleff, J.; Terrett, J. A.; Cuthbertson, J. D.; MacMillan, D. W. C. Native functionality in triple catalytic cross-coupling: sp³ C–H bonds as latent nucleophiles. *Nature*, **2016**, *352*, 1304–1308. (h) Aye, Y.; Kalvet, I.; Schoenebeck, F.; Rovis, T. Direct α-alkylation of primary amines enabled by CO_2 and electrostatics. *Nat. Chem.* **2018**, *10*, 1037–1041.

(9) Trowbridge, A.; Reich, D.; Gaunt, M. J. Multicomponent synthesis of tertiary alkylamines by photocatalytic olefin hydroaminoalkylation. *Nature* **2018**, *561*, 522–527.

(10) Aurrecoechea, J. M. Suero, R. Recent developments in cyclization reactions of α-amino radicals. *Arkivoc*, **2004**, *xiv*, 10–35.

(11) Maity, S.; Flowers II, R. A. Mechanistic study and development of catalytic reactions of Sm(II). *J. Am. Chem. Soc.* **2019**, 141, 3207–3216.

(12) Jung, S.; Kang, Y.; Kim, H.-S.; Kim, Y.-H.; Lee, C.-L.; Kim, J.-J.; Lee, S.-K.; Kwon, S.-K. Effect of substitution of methyl groups on the luminescence performance of Ir[III] complexes: Preparation, structures, electrochemistry, photophysical properties and their applications in organic light-emitting diodes (OLEDs). *Eur. J. Inorg. Chem.* **2004**, *2004*, 3415–3423.

(13) See supporting information.

(14) Bittermann, H.; Böckler, F.; Einsiedel, J.; Gmeiner, P. A highly practical RCM approach towards a molecular building kit of spirocyclic reverse turn mimics. *Chem. Eur. J.* **2006**, *12*, 6315–6322.

(15) Lai. J. Hindered amines. 3,3,5,5-Tetrasubstituted-2-oxomorpholines and derivatives. *Synthesis* **1984**, 122–123.

(16) Corey, E. J.; Gross, A. W. Methods for the synthesis of chiral hindered amines. *J. Org. Chem.* **1985**, *50*, 5391–5393.

(17) Nosik, P. S.; Gerasov, A. O.; Boiko, R. O.; Rusanov, E.; Ryabukhin, S. V.; Grygorenko, O. O.; Volochnyuk, D. M. Gram-scale synthesis of amines bearing a *gem*-difluorocyclopropane moiety. *Adv. Synth. Catal.* **2017**, *359*, 3126–3136.

The image part with relationship ID rId28 was not found in the file.

The image part with relationship ID rId28 was not found in the file.